Fermi National Accelerator Laboratory

FERMILAB-Pub-93/361-E

E687

A Measurement of the Cabibbo-Suppressed Decays $D^0 \to \pi^-\pi^+$ and $D^0 \to K^-K^+$

P.L. Frabetti et al
The E687 Collaboration

Fermi National Accelerator Laboratory
P.O. Box 500, Batavia, Illinois 60510

November 1993

Submitted to *Physics Letters B*

Operated by Universities Research Association Inc. under Contract No. DE-AC02-76CHO3000 with the United States Department of Energy

Disclaimer

A measurement of the Cabibbo-suppressed decays $D^0 \to \pi^-\pi^+$ and $D^0 \to K^-K^+$

P. L. Frabetti

Dip. di Fisica dell'Università and INFN - Bologna, I-40126 Bologna, Italy

H. W. K. Cheung, J. P. Cumalat, C. Dallapiccola [a], J. F. Ginkel, S. V. Greene, W. E. Johns, M. S. Nehring

University of Colorado, Boulder, CO 80309, USA

J. N. Butler, S. Cihangir, I. Gaines, P. H. Garbincius, L. Garren, S. A. Gourlay, D. J. Harding, P. Kasper, A. Kreymer, P. Lebrun, S. Shukla, M. Vittone

Fermilab, Batavia, IL 60510, USA

S. Bianco, F. L. Fabbri, S. Sarwar, A. Zallo

Laboratori Nazionali di Frascati dell'INFN, I-00044 Frascati, Italy

R. Culbertson, R. W. Gardner, R. Greene, J. Wiss

University of Illinois at Urbana-Champaign, Urbana,IL 61801

G. Alimonti, G. Bellini, B. Caccianiga, L. Cinquini [b], M. Di Corato, M. Giammarchi, P. Inzani, F. Leveraro, S. Malvezzi [c], D. Menasce, E. Meroni, L. Moroni, D. Pedrini, L. Perasso, A. Sala, S. Sala, D. Torretta [d]

Dip. di Fisica dell'Università and INFN - Milano, I-20133 Milan, Italy

D. Buchholz, D. Claes [e], B. Gobbi, B. O'Reilly,

Northwestern University, Evanston, IL 60208, USA

J. M. Bishop, N. M. Cason, C. J. Kennedy [f], G. N. Kim, T. F. Lin, D. L. Puseljic, R. C. Ruchti, W. D. Shephard, J. A. Swiatek, Z. Y. Wu

University of Notre Dame, Notre Dame, IN 46556, USA

V. Arena, G. Boca, C. Castoldi, G. Gianini, S. P. Ratti, C. Riccardi, P. Vitulo

Dip. di Fisica Nucleare e Teorica and INFN - Pavia, I-27100 Pavia, Italy

A. Lopez

University of Puerto Rico at Mayaguez, Puerto Rico

G. P. Grim, V. S. Paolone, P. M. Yager

University of California-Davis, Davis, CA 95616

J. R. Wilson

University of South Carolina, Columbia, SC 29208

P. D. Sheldon

Vanderbilt Univeristy, Nashville, Tenn.,TN 37235 USA

F. Davenport

University of North Carolina-Asheville, Asheville, NC 28804

J. F. Filaseta

Northern Kentucky University, Highland Heights, KY 41076

G.R. Blackett, M. Pisharody, T. Handler

University of Tennessee, Knoxville, TN 37996 USA

B. G. Cheon, J. S. Kang, K. Y. Kim

Korea University, Seoul 136-701, Korea

Abstract

We report a measurement of the relative branching ratio of two Cabibbo-suppressed decay modes: $D^0 \to \pi^-\pi^+$ and $D^0 \to K^-K^+$. The data were accumulated in the 1990-1991 fixed target run of Fermilab high energy photoproduction experiment E687 . The branching ratios of these modes relative to the Cabibbo-allowed decay $D^0 \to K^-\pi^+$ are also presented. The relative branching ratios are measured to be : $\frac{\Gamma(D^0 \to KK)}{\Gamma(D^0 \to \pi\pi)} = 2.53 \pm 0.46 \pm 0.19$, $\frac{\Gamma(D^0 \to KK)}{\Gamma(D^0 \to K\pi)} = 0.109 \pm 0.007 \pm 0.009$, and $\frac{\Gamma(D^0 \to \pi\pi)}{\Gamma(D^0 \to K\pi)} = 0.043 \pm 0.007 \pm 0.003$.

1. Introduction

Two-body decays of charm mesons offer a unique opportunity to investigate the hadronic structure of charm weak decay in simple unique states, in contrast with multibody decays where resonances may be present. A particular interest in the decay modes $D^0 \to \pi^-\pi^+$ and $D^0 \to K^-K^+$ stems from the question: why is $D^0 \to \pi^-\pi^+$ decay more suppressed than $D^0 \to K^-K^+$? The observed ratio $\frac{\Gamma(D^0 \to KK)}{\Gamma(D^0 \to \pi\pi)}$ is ~ 2.5 [1].

These two decay modes can proceed through similar diagrams so that with no SU(3) flavour symmetry breaking the ratio is 1; including phase space difference for real π and K masses makes the ratio 0.86. Theoretical models [2], taking into account SU(3) breaking, predict a ratio on the order of 1.4, still smaller than observed. More recently, several approaches have been proposed to explain the large experimental value for this ratio. One involves final state interactions which shift the relative rates into the various two body channels differently for $\pi\pi$ and KK final states altering the ratio [3]. Another invokes penguin diagrams which interfere constructively with the spectator decay for KK but destructively for $\pi\pi$ [4]. A third relies on a non-perturbative algebraic approach [5].

Precise measurements of all the two body decay modes will help to discriminate among models as those mentioned above. This will help our understanding of the Standard Model predictions for $D^0 - \overline{D}^0$ mixing through long range mechanisms, which depend on SU(3) symmetry-breaking to become non-zero. *Direct CP* violation may be caused by the interference of penguin diagrams and spectator diagrams and also requires strong phase shifts. Such CP asymmetries are also largest for decay modes which are suppressed, so an understanding of various suppression mechanisms can help to reveal promising states for CP studies in charm [6].

Fermilab experiment E687 has recorded and analyzed one of the largest samples now available for $D^0 \to \pi^-\pi^+$ and $D^0 \to K^-K^+$ and also for $D^0 \to K^-\pi^+$. (Throughout this paper the charge conjugate state is implied when a decay mode of a specific charge is stated.) Our results provide improved measurements of these decays and strengthen the evidence for a large $\frac{\Gamma(D^0 \to KK)}{\Gamma(D^0 \to \pi\pi)}$ ratio.

E687 is a high energy photoproduction experiment designed to study the physics of heavy quarks. The average tagged-photon energy was about 220 GeV and approximately 500 million triggers were recorded on tape during the 1990-91 run. The E687 spectrometer and reconstruction procedures have been described in detail elsewhere [7].

In this analysis two experimental techniques are extremely important: particle identification and event topology discrimination. The charged particle identification, performed with a system of three multicell Čerenkov counters operating in threshold mode, is able to separate kaons from pions over the momentum range 4.5 to 61 GeV/c. Tracks are reconstructed using a sophisticated microvertex detector composed of 12 planes of silicon microstrips with a resolution of 9 μm in the transverse plane, allowing the identification and separation of charm production and decay vertices.

A first selection was performed on the whole sample: it required satisfactory confidence levels ($C.L. \geq 1\%$) for a primary vertex located in the target and for a secondary vertex consisting of two well reconstructed tracks of opposite charge with an invariant mass in the range 1.65 to 2.05 GeV/c^2 for track combinations consistent with $\pi^-\pi^+$, K^-K^+, or $K^-\pi^+$ hypotheses. This selection reduced the sample from 500 million to $\sim$ 15 million events.

2. Analysis of $D^0 \to \pi^-\pi^+$, $D^0 \to K^-K^+$ and $D^0 \to K^-\pi^+$ decays

Particle identification requirements for each decay mode have been chosen to optimize signal quality. In addition to large combinatorial backgrounds, $D^0 \to \pi^-\pi^+$ decays are difficult to isolate because of a large reflection from $D^0 \to K^-\pi^+$ decays when the kaon is misidentified as a pion. In order to reduce this reflection and limit the background, both pions for this decay are required to be identified unambiguously (i.e. to have the unique light pattern expected for a pion) by the Čerenkov system. For $D^0 \to K^-K^+$ decays less stringent requirements are needed. There is still a reflection from $D^0 \to K^-\pi^+$ decays, but requiring that both kaons be identified as kaon definite or kaon/proton ambiguous is sufficient to eliminate the reflected peak almost completely. In the $D^0 \to K^-\pi^+$ analysis still less restrictive Čerenkov cuts are employed because the only significant background is combinatoric. The kaon is allowed to be kaon definite or kaon/pion ambiguous or kaon/proton ambiguous, while the pion need only be consistent with the Čerenkov pion hypothesis.

After pairs of candidate tracks for the decay are selected, the event is then reconstructed with a *candidate driven vertex algorithm* described in detail elsewhere [8]. Briefly, a secondary vertex is formed from the candidate tracks, a *seed* track is formed using the candidate momentum vectors, and a primary vertex is constructed from other tracks in the event which intersect the *seed* track. The confidence levels of the primary vertex (CLP) and secondary vertex (CLS) and two estimators of the relative isolation of these vertices are returned by the algorithm; the first estimator ($ISO1$) is the confidence level that tracks forming the secondary vertex might come from the primary vertex, the second estimator ($ISO2$) is the confidence level that other tracks in the event might be associated with the secondary vertex. This set of four variables provides a good measure of the topological configuration of the event, so that appropriate cuts on them reject the combinatorial background effectively.

The final important cut is on the significance of detachment between the primary and secondary vertices, L/σ_L, where L is the distance between the vertices and σ_L is its error. We require $\mathrm{L}/\sigma_L \geq 8$ to optimize the signal to noise ratio for the $D^0 \to \pi^-\pi^+$ sample.

In the present analysis common vertexing cuts were applied for all the decay modes of interest to reduce systematic errors. The cuts ($CLP \geq 2\%$, $CLS \geq 2\%$, $ISO1 \leq 30\%$, $ISO2 \leq 0.1\%$ and $\mathrm{L}/\sigma_L \geq 8$) have been chosen to give the best signal to noise ratio for data in conjunction with the best agreement between the mass and the width of the signal and the corresponding Monte Carlo simulations.

Using the set of cuts just described we obtain the mass plots for $\pi^-\pi^+$, K^-K^+, and $K^-\pi^+$, shown in Fig.1, Fig.2, and Fig.3 respectively.

In Fig. 1, the $\pi^-\pi^+$ mass plot shows a broad peak to the left of the D^0 signal due to surviving contamination from $D^0 \to K^-\pi^+$ events. The distribution has been fitted with a function including a first Gaussian for the signal, with mass fixed at the nominal value [1]

($M = 1.8645$ GeV/c^2) and width fixed at a value from Monte Carlo simulations ($\sigma = 13.63$ MeV/c^2), a second Gaussian for the fitted portion of the reflection peak, and a second order polynomial for the remaining background. The mass and width are fixed for this state because this gives somewhat more stable results than letting them float due to the presence of the large reflection nearby. The result does not depend crucially on this. A least squares fit with this function gives a signal of 177 ± 30 $\pi^-\pi^+$ events.

The K^-K^+ signal, shown in Fig. 2, has a better signal to noise ratio because the Čerenkov identification requirements on the two kaons eliminates much combinatorial background. A least squares fit with a function similar to that for the $\pi^-\pi^+$ fit, except that the signal mass and width were not fixed, gives a signal of 581 ± 37 K^-K^+ events; note that the fit function still includes a second Gaussian to describe residual reflection from $D^0 \to K^-\pi^+$ with the pion misidentified.

The $K^-\pi^+$ mass plot of Fig. 3 is fitted with a Gaussian for the signal (mass and width not fixed) and a second order polynomial for the background. The fit gives a signal of 11048 ± 145 $K^-\pi^+$ events.

In the fit procedure the mass range was from 1.72 to 2.04 GeV/c^2; the lower limit was chosen to avoid contamination from decays involving either an additional π^0 (for example $\rho^+\pi^-$ or $\pi^+\pi^-\pi^0$) or charged pions outside the spectrometer acceptance. In the K^-K^+ and $K^-\pi^+$ fits, the fitted D^0 mass was in good agreement with the world average [1], and the width was in good agreement with results from our Monte Carlo simulation of the spectrometer.

3. Relative Branching Ratios

In the evaluation of relative branching ratios the yields from the fits must be corrected for detection efficiencies, which differ because of differences in both spectrometer acceptance (due to different Q values for the decay modes) and Čerenkov identification efficiency. The global efficiencies, determined from Monte Carlo simulation studies, are: $\epsilon_{\pi\pi} = 0.0191 \pm 0.0005$, $\epsilon_{KK} = 0.0247 \pm 0.0006$ and $\epsilon_{K\pi} = 0.0514 \pm 0.0009$.

Using the previous results and systematic errors to be discussed below we obtain the following values for relative branching ratios: $\frac{\Gamma(D^0 \to KK)}{\Gamma(D^0 \to \pi\pi)} = 2.53 \pm 0.46 \pm 0.19$, $\frac{\Gamma(D^0 \to KK)}{\Gamma(D^0 \to K\pi)} = 0.109 \pm 0.007 \pm 0.009$, and $\frac{\Gamma(D^0 \to \pi\pi)}{\Gamma(D^0 \to K\pi)} = 0.043 \pm 0.007 \pm 0.003$. In Table 1 these new results are compared with results from earlier experiments [8-14]. Where two errors are shown, the first is statistical and the second is systematic.

We consider four significant contributions to our systematic errors: uncertainty in the Monte Carlo simulation of the Čerenkov system, uncertainty due to hadronic interactions of secondaries in the target, variation in yields due to different background parametrizations, and the finite statistics of Monte Carlo simulations. These contributions have been separately evaluated for each decay mode and the quoted systematic errors are obtained by adding the four terms in quadrature.

Our final results have been submitted to a number of further checks. The first is the stability of the branching ratios as a function of the L/σ_L cut, the most powerful tool in extracting the charm signal from the background. This stability is illustrated in Fig. 4 where the variation of the three branching ratios with the L/σ_L cut is shown. Due to the small $D^0 \to \pi^-\pi^+$ sample, the fluctuations are larger in Figs. 4a and 4c, but are well within the statistical errors.

The final numbers have also been tested by modifying each of the other analysis cuts individually; the results were always consistent within errors. Various other studies were made to try to decrease backgrounds. These included requiring that the D^0 mesons in the sample come from the decay of $D^{*\pm}$ (D^* tagging), cutting on the ratio of the momentum of a decay particle to the momentum of the D^0 to eliminate combinatorial background connected with unassociated tracks of very high or low momenta, etc. In each case these studies produced results for the branching ratios consistent with the quoted values, but did not result in a significant reduction in the errors.

A final check was made by using a different algorithm for event reconstruction, a *stand alone vertex algorithm* [15] instead of the *candidate driven vertex algorithm* described previously. This algorithm finds the best topological configuration for an event independent of physics constraints such as charge and strangeness. The $\pi^-\pi^+$ mass plot obtained with this technique is shown in Fig. 5. This algorithm is inherently inefficient for short decay paths but the signals are quite clean. The branching ratios obtained with the *stand alone vertex algorithm* are: $\frac{\Gamma(D^0\to KK)}{\Gamma(D^0\to\pi\pi)} = 2.60 \pm 0.43 \pm 0.25$, $\frac{\Gamma(D^0\to KK)}{\Gamma(D^0\to K\pi)} = 0.114 \pm 0.009 \pm 0.009$ and $\frac{\Gamma(D^0\to\pi\pi)}{\Gamma(D^0\to K\pi)} = 0.043 \pm 0.006 \pm 0.004$, in excellent agreement with our values of Table 1.

4. Conclusions

We have measured the relative branching ratios $D^0 \to K^-K^+ / D^0 \to \pi^-\pi^+$, $D^0 \to K^-K^+ / D^0 \to K^-\pi^+$, and $D^0 \to \pi^-\pi^+ / D^0 \to K^-\pi^+$. As shown in Table 1, these new E687 values are in agreement with almost all the previous measurements. (This concordance is due primarily to the large statistical errors for the different measurements.)

Our measurement confirms a large value for the ratio $D^0 \to K^-K^+ / D^0 \to \pi^-\pi^+$ and is thus consistent with several recent theoretical models [3,4,5].

We wish to acknowledge the assistance of the staff of Fermi National Accelerator Laboratory, the INFN of Italy, and the staffs of the physics departments of the collaborating institutions. This research was supported in part by the U.S. National Science Foundation, the U.S. Department of Energy, the Italian Istituto Nazionale di Fisica Nucleare and Ministero dell'Università e della Ricerca Scientifica, and the Korean Science and Engineering Foundation.

TABLE 1. Branching ratios: Comparison with the other experiments

Experiment	$\frac{\Gamma(D^0\to K^-K^+)}{\Gamma(D^0\to\pi^-\pi^+)}$	$\frac{\Gamma(D^0\to K^-K^+)}{\Gamma(D^0\to K^-\pi^+)}$	$\frac{\Gamma(D^0\to\pi^-\pi^+)}{\Gamma(D^0\to K^-\pi^+)}$
Mark II [8]	3.4 ± 1.8	0.113 ± 0.030	0.033 ± 0.015
Mark III [9]	3.7 ± 1.4	0.122 ± 0.018	$0.033 \pm 0.010 \pm 0.006$
ARGUS [10]	2.5 ± 0.7	$0.10 \pm 0.02 \pm 0.01$	$0.040 \pm 0.007 \pm 0.006$
CLEO [11]	$2.35 \pm 0.37 \pm 0.28$	$0.117 \pm 0.010 \pm 0.007$	$0.035 \pm 0.003 \pm 0.002$
NA14 [12]	-	0.16 ± 0.05	-
E691 [13]	$1.95 \pm 0.34 \pm 0.22$	$0.107 \pm 0.010 \pm 0.009$	$0.055 \pm 0.008 \pm 0.005$
WA82 [14]	$2.23 \pm 0.81 \pm 0.46$	$0.107 \pm 0.029 \pm 0.015$	$0.048 \pm 0.013 \pm 0.008$
E687	$2.53 \pm 0.46 \pm 0.19$	$0.109 \pm 0.007 \pm 0.009$	$0.043 \pm 0.007 \pm 0.003$

REFERENCES

[a] Present address: University of Maryland, College Park, MD, 20742,USA

[b] Present address: University of Colorado, Boulder, CO 80309, USA

[c] Present address: Dip. di Fisica Nucleare e Teorica and INFN - Pavia, I-27100 Pavia, Italy

[d] Present address: Fermilab, Batavia, IL 60510, USA.

[e] Present address: State University of New York, Stony Brook, NY 11794, USA.

[f] Present address: Yale University, New Haven, CN 06511, USA.

[1] Particle Data Group, K. Hikasa et al., Phys. Rev. D 45 No. 11 (1992) Pt. II.

[2] A. Buras *et al.*, Nucl.Phys. B268 (1986) 16.

M. Bauer *et al.*, Z. Phys. C 34 (1987) 103.

[3] A. N. Kamal *et al.*, Phys. Rev. D 35 (1987) 3515.

A. N. Kamal *et al.*, Phys. Rev. D 36 (1987) 3510.

A. Czarnecki *et al.*, Z. Phys. C 54 (1992) 411.

L. L. Chau *et al.*, Phys. Lett. B 280 (1992) 281.

[4] M. Gluck, Phys. Lett. B 88 (1979) 145.

J. Finjord, Nucl. Phys. B 181 (1981) 74.

[5] K. Terasaki *et al.*, Phys. Rev. D 38 (1988) 132.

[6] I. Bigi, private communication, 8/93.

[7] P. L. Frabetti *et al.*, Nucl. Instrum. Methods A 320 (1992) 519.

[8] G. S. Abrams *et al.*, Phys. Rev. Lett. 43 (1979) 481.

[9] R. M. Baltrusaitis *et al.*, Phys. Rev. Lett. 55 (1985) 150.

[10] H. Albrecht *et al.*, Z. Phys. C 46 (1990) 9.

[11] J. Alexander *et al.*, Phys. Rev. Lett. 65 (1990) 1184.

M. Selen *et al.*, Phys. Rev. Lett. 71 (1993) 1973, for the value of $\frac{\Gamma(D^0 \to \pi\pi)}{\Gamma(D^0 \to K\pi)}$.

[12] M. P. Alvarez *et al.*, Z. Phys. C 50 (1991) 11.

[13] J. C. Anjos *et al.*, Phys. Rev. D 44 (1991) R3371.

[14] M.Adamovich *et al.*, Phys. Lett. B 280 (1992) 163.

[15] P. L. Frabetti *et al.*, Phys. Lett. B 281 (1992) 167.

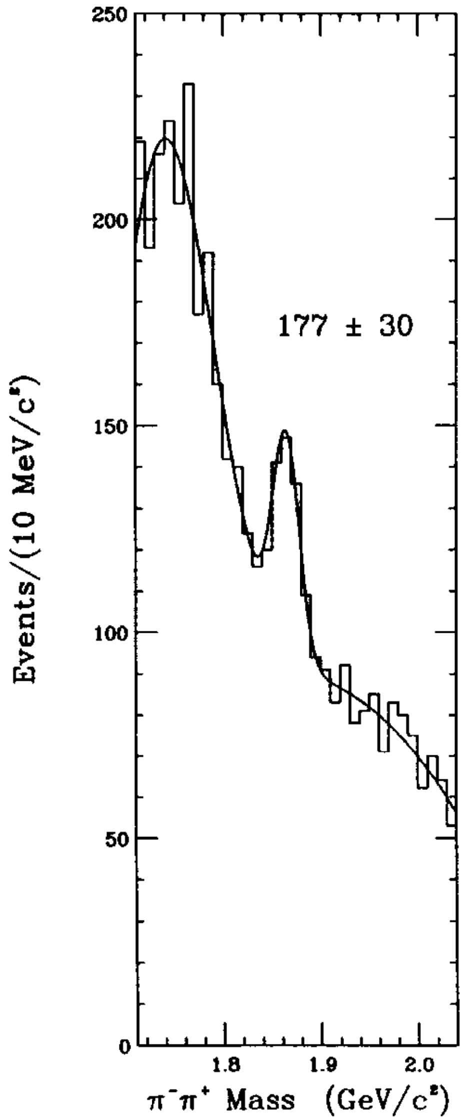

Fig.1 $\pi^-\pi^+$ invariant mass distribution. The fit (solid curve) is described in the text.

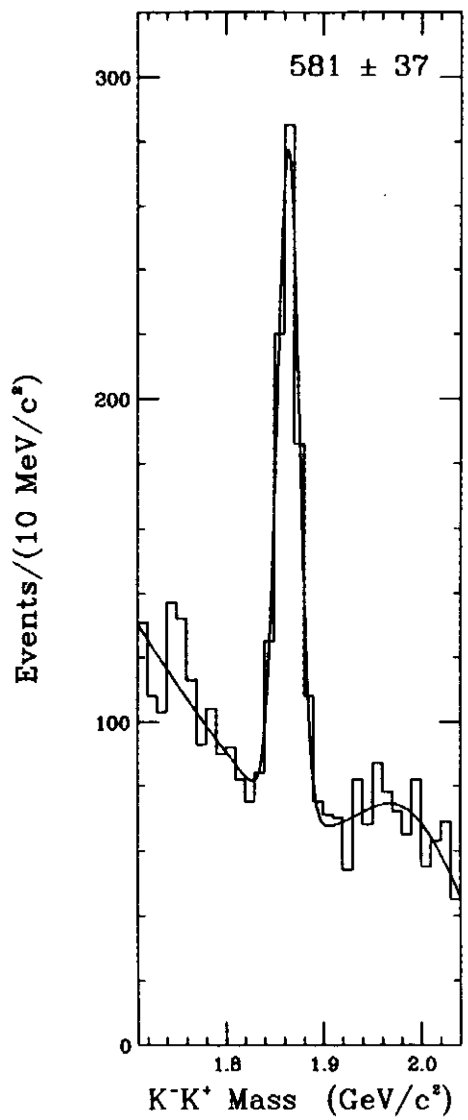

Fig.2 K^-K^+ invariant mass distribution. The fit (solid curve) is described in the text.

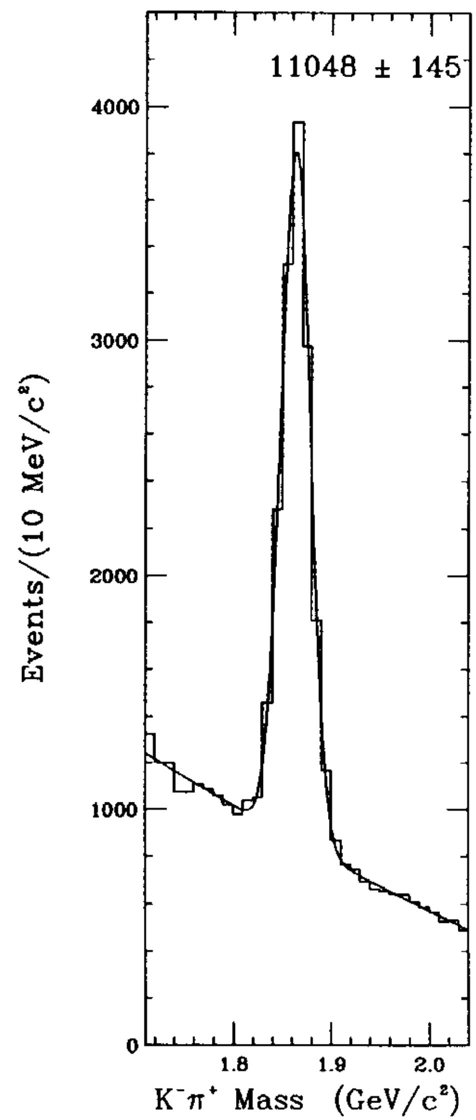

Fig.3 $K^-\pi^+$ invariant mass distribution. The fit (solid curve) is described in the text.

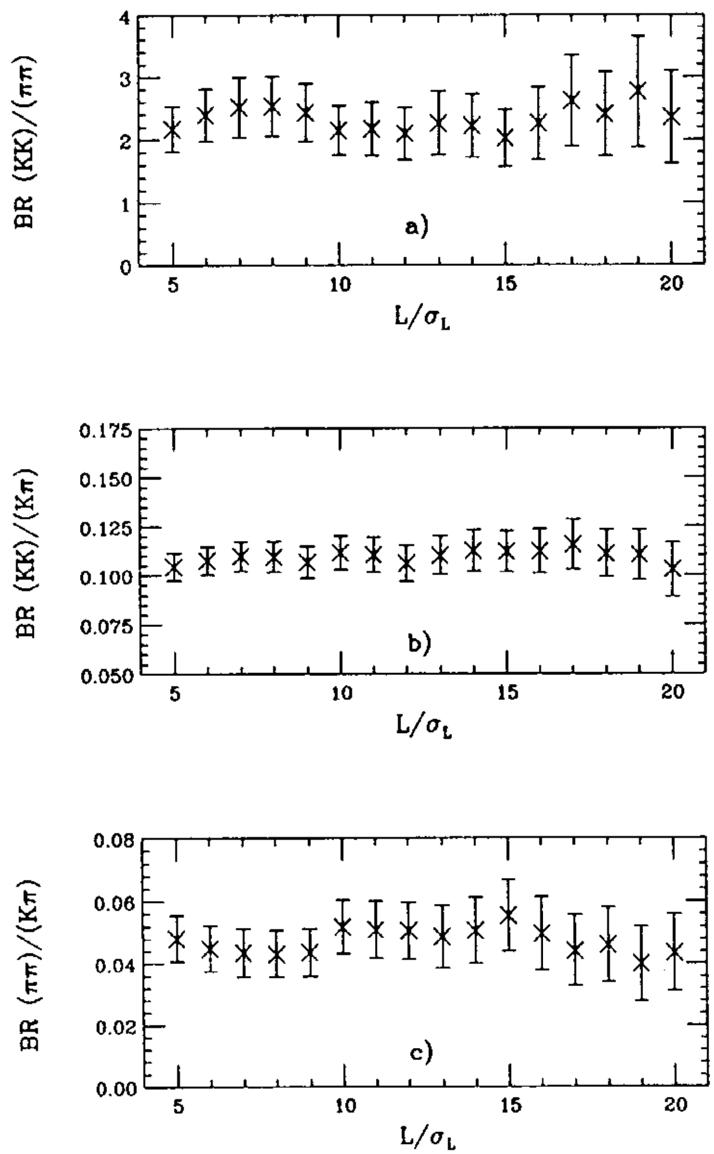

Fig.4 Branching ratios a) $\frac{\Gamma(D^0\to KK)}{\Gamma(D^0\to\pi\pi)}$, b) $\frac{\Gamma(D^0\to KK)}{\Gamma(D^0\to K\pi)}$, and c) $\frac{\Gamma(D^0\to\pi\pi)}{\Gamma(D^0\to K\pi)}$ as a function of the L/σ_L cut (see text).

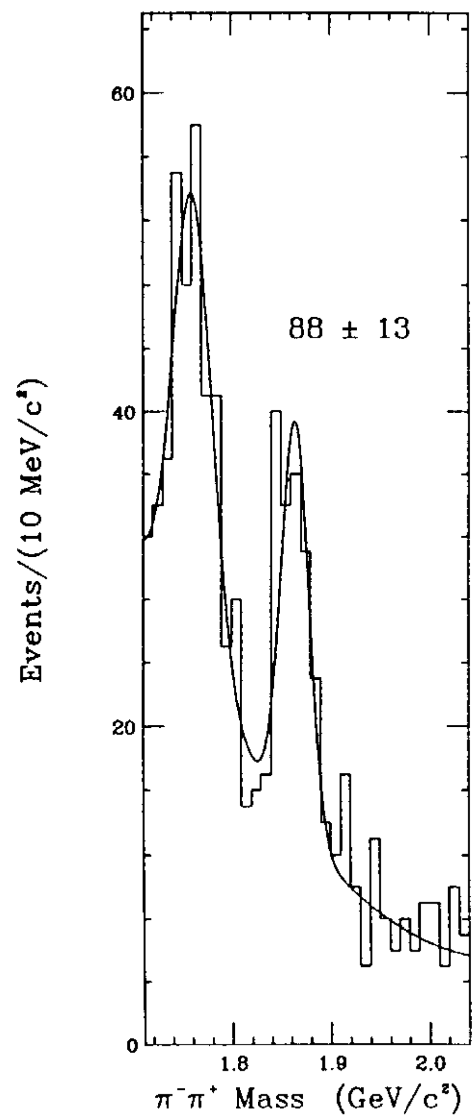

Fig.5 Alternative $\pi^-\pi^+$ invariant mass distribution (with superimposed fit) obtained with the *stand alone vertex algorithm* as described in the text.